



## PAPER

[View Article Online](#)  
[View Journal](#)

Cite this: DOI: 10.1039/d5dt01410g

Comparison of catalytic activities of aluminum complexes with sulfur and oxygen containing ligands for the ring-opening polymerization of  $\epsilon$ -caprolactoneTzu-Yu Lin,<sup>a</sup> Yu-Chi Liou,<sup>b</sup> Taoufik Ben Halima,<sup>c</sup> Shih-Ya Huang,<sup>a</sup> Rajiv Kamaraj,<sup>a</sup> Hsi-Ching Tseng,<sup>d</sup> Shangwu Ding,<sup>a,b</sup> Hsuan-Ying Chen <sup>\*a,b,e,f</sup> and Chien-Ming Lee <sup>\*g</sup>

A series of aluminum complexes bearing various ligands, including *tert*-butanolate, *tert*-butyl thiolate, 2,6-dimethylphenolate, 2,6-dimethylbenzenethiolate, 2,6-di-*tert*-butyl-4-methylphenolate, 2,6-di-trimethylsilylbenzenethiolate, furan-2-ylmethanolate, thiophen-2-ylmethanolate, pyridin-2-olate, pyridine-2-thiolate, quinolin-8-olate, and quinoline-8-thiolate were synthesized and assessed for their catalytic activity in the ring-opening polymerization of  $\epsilon$ -caprolactone (CL). Polymerization results revealed that **S<sup>Si</sup>-Al** exhibited a significantly higher catalytic activity ([CL] : [S<sup>Si</sup>-Al] : [BnOH] = 100 : 1 : 2; [CL] = 2 M; conv. = 92% at 25 °C after 35 min with  $k_{\text{obs}} = 0.0733 \text{ min}^{-1}$ ) compared to **O<sup>BHT</sup>-Al** ( $k_{\text{obs}} = 0.0196 \text{ min}^{-1}$ ), with a 3.7-fold increase in  $k_{\text{obs}}$  values. Other sulfur-containing Al complexes also demonstrated superior catalytic performance compared to their oxygen-containing counterparts: 7.1-fold (**S<sup>dm</sup>-Al** vs. **O<sup>dm</sup>-Al**), 2.9-fold (**S<sup>tBu</sup>-Al** vs. **O<sup>tBu</sup>-Al**), 10.0-fold (**S<sup>Py</sup>-Al** vs. **O<sup>Py</sup>-Al**), 2.2-fold (**S<sup>thio</sup>-Al** vs. **O<sup>fu</sup>-Al**), and 16.4-fold (**S<sup>Qu</sup><sub>2</sub>-Al** vs. **O<sup>Qu</sup><sub>2</sub>-Al**). Although **S<sup>tBu</sup>-Al** demonstrated the highest catalytic activity, its capacity to control CL polymerization was found to be limited. In contrast, the Al complexes bearing quinoline type ligands revealed the lowest catalytic activity. **S<sup>dm</sup>-Al** revealed the second highest catalytic activity and provided good controllable CL polymerization. These findings demonstrate that incorporating sulfur into ligand structures may enhance the catalytic performance of Al complexes in CL ring-opening polymerization.

Received 16th June 2025,  
Accepted 4th August 2025

DOI: 10.1039/d5dt01410g

rsc.li/dalton

## Introduction

Petrochemical-based plastics are extensively used due to their light weight and durable properties, making them essential for manufacturing everyday materials. However, their durability also contributes to environmental pollution, as they are not

readily biodegradable upon disposal.<sup>1</sup> To address this global challenge, eco-friendly alternatives, such as poly- $\epsilon$ -caprolactone (PCL),<sup>2</sup> have been developed. Furthermore, PCL-based materials are notable for their permeability<sup>3</sup> and biocompatibility,<sup>4</sup> rendering them suitable for diverse applications.<sup>5</sup> The main method of PCL synthesis is the ring-opening polymerization (ROP) of  $\epsilon$ -caprolactone (CL),<sup>6</sup> typically catalyzed by metal complexes. In this mechanism, the metal center acts as a Lewis acid, coordinating with CL and thereby activating it for nucleophilic attack *via* an initiator<sup>6c,e,f,7</sup> (Scheme 1). However, side reactions such as intra- and intermolecular transesterification<sup>6c</sup> during polymerization can compromise molecular mass control and dispersity. To suppress transesterification, bulky ligands are often employed to limit carbonyl coordination along the polymer chain. Nonetheless, these bulky ligands may also hinder the monomer's access to the metal center. Therefore, rational ligand design is crucial for optimizing the spatial and electronic environments around the metal catalyst, enhancing both activity and control.

Aluminum complexes<sup>8</sup> are widely used as catalysts in the CL ROP due to their high catalytic activity, excellent monomer

<sup>a</sup>Department of Medicinal and Applied Chemistry, Drug Development and Value Creation Research Center, Kaohsiung Medical University, Kaohsiung, Taiwan, 80708, Republic of China. E-mail: hchen@kmu.edu.tw; Fax: +886-7-3125339;

Tel: +886-7-3121101-2585

<sup>b</sup>Department of Chemistry, National Sun Yat-Sen University, Kaohsiung, Taiwan, 80424, Republic of China

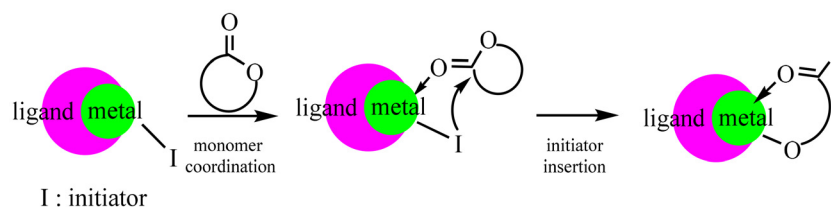
<sup>c</sup>Department of Chemistry & Biomolecular Sciences, University of Ottawa, Ottawa, Canada

<sup>d</sup>College of Science Instrumentation Center, National Taiwan University, Taipei, Taiwan, 106319, Republic of China

<sup>e</sup>Department of Medical Research, Kaohsiung Medical University Hospital, Kaohsiung 80708, Taiwan, Republic of China

<sup>f</sup>National Pingtung University of Science and Technology, Pingtung, Taiwan 91201, Republic of China

<sup>g</sup>Department of Applied Science, National Taitung University, Taitung, Taiwan 950, Republic of China



**Scheme 1** Coordination–insertion mechanism of cyclic ester polymerization.

conversion to PCL, and straightforward synthesis procedures. The design of ligands plays a crucial role, as different substituents<sup>7a,9</sup> can modulate the electron density around the metal center, thereby influencing the catalytic performance of the complex.

Our research aims to explore and design new strategies to enhance the catalytic efficiency of Al catalysts in CL ROP. Recent comparative studies have investigated the catalytic performance of aluminum complexes bearing various ligand frameworks such as *N,O*-Schiff base vs. *N,S*-thioSchiff base<sup>10</sup> (Fig. 1A), *N,N'*-diaryldioxalamidate vs. *N,N'*-diaryldithiooxalamidate<sup>11</sup> (Fig. 1B), amidate vs. thioamidate<sup>8l</sup> (Fig. 1C), and  $\beta$ -ketiminate vs.  $\beta$ -thioketiminate<sup>8m</sup> (Fig. 1D). Given the larger atomic radius of sulfur compared to oxygen, ligands

containing sulfur, such as *N,S*-thioSchiff base, *N,N'*-diaryldithiooxalamidate, and  $\beta$ -thioketiminate, tend to reduce steric repulsion at the highest transition state during CL polymerization. This results in lower activation energy barriers and consequently higher catalytic activity than those of their oxygen-containing analogues. In the case of eight-membered Al complexes bearing amidate and thioamidate, those with thioamidate adopt a four-membered transition state with a more open coordination geometry, characterized by a smaller N–Al–S bond angle and lower potential energy. In contrast, amidate-containing complexes retain the more hindered eight-membered transition state with a relatively larger N–Al–O bond angle, which is less conducive for catalysis. Zaitsev's group<sup>12</sup> also reported that sulfur-containing Al

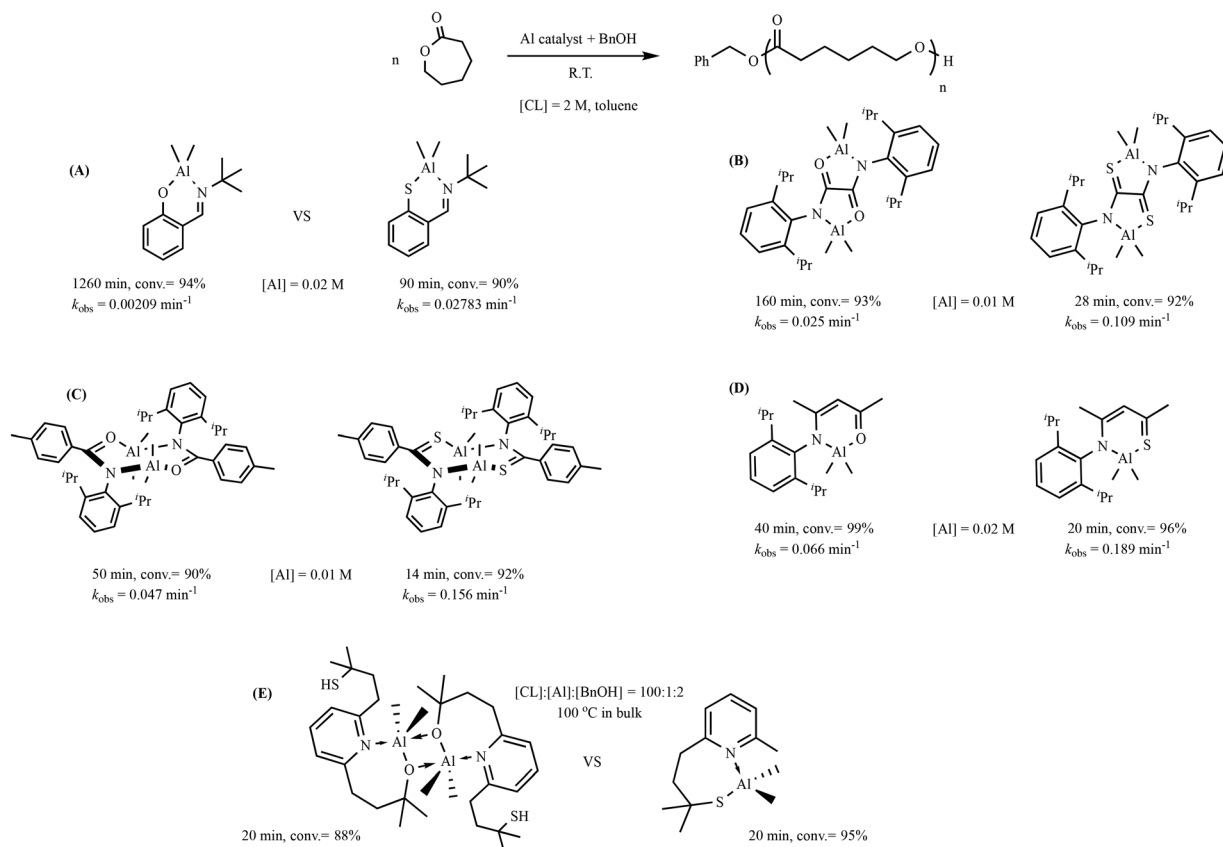


**Fig. 1** CL polymerization performed using Al complexes bearing ligands containing sulfur and oxygen atoms, including (A) Schiff base, (B) *N,N'*-diaryldioxalamidate, (C) amidate, (D) ketiminate, and (E) 2-methyl-4-(pyridin-2-yl)butan-2-olate.

catalysts exhibit higher catalytic activity for CL polymerization compared to oxygen-containing Al catalysts (Fig. 1E). This is attributed to the higher electronegativity of the oxygen atom, which, in oxygen-containing complexes, results in a stronger interaction between the initiator BnO group and the Al center, thereby slowing down the initiation of the BnO group, which is the rate-determining step in ROP. In contrast, for sulfur-containing ligands, the BnO group can more easily initiate from the Al center to the CL. Furthermore, due to the larger atomic radius of sulfur compared to oxygen, the sulfur-containing complexes are more open in structure.

We sought to investigate whether Al complexes bearing sulfur-containing ligands demonstrate superior catalytic activity in CL ROP relative to those featuring oxygen-containing ligands. In this study, a series of aluminum complexes were synthesized using both sulfur- and oxygen-containing ligands (Scheme 2), and their catalytic performance in CL polymerization was systematically evaluated.

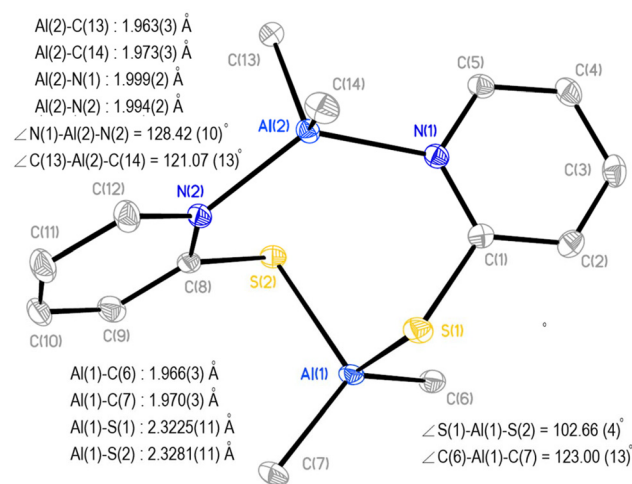
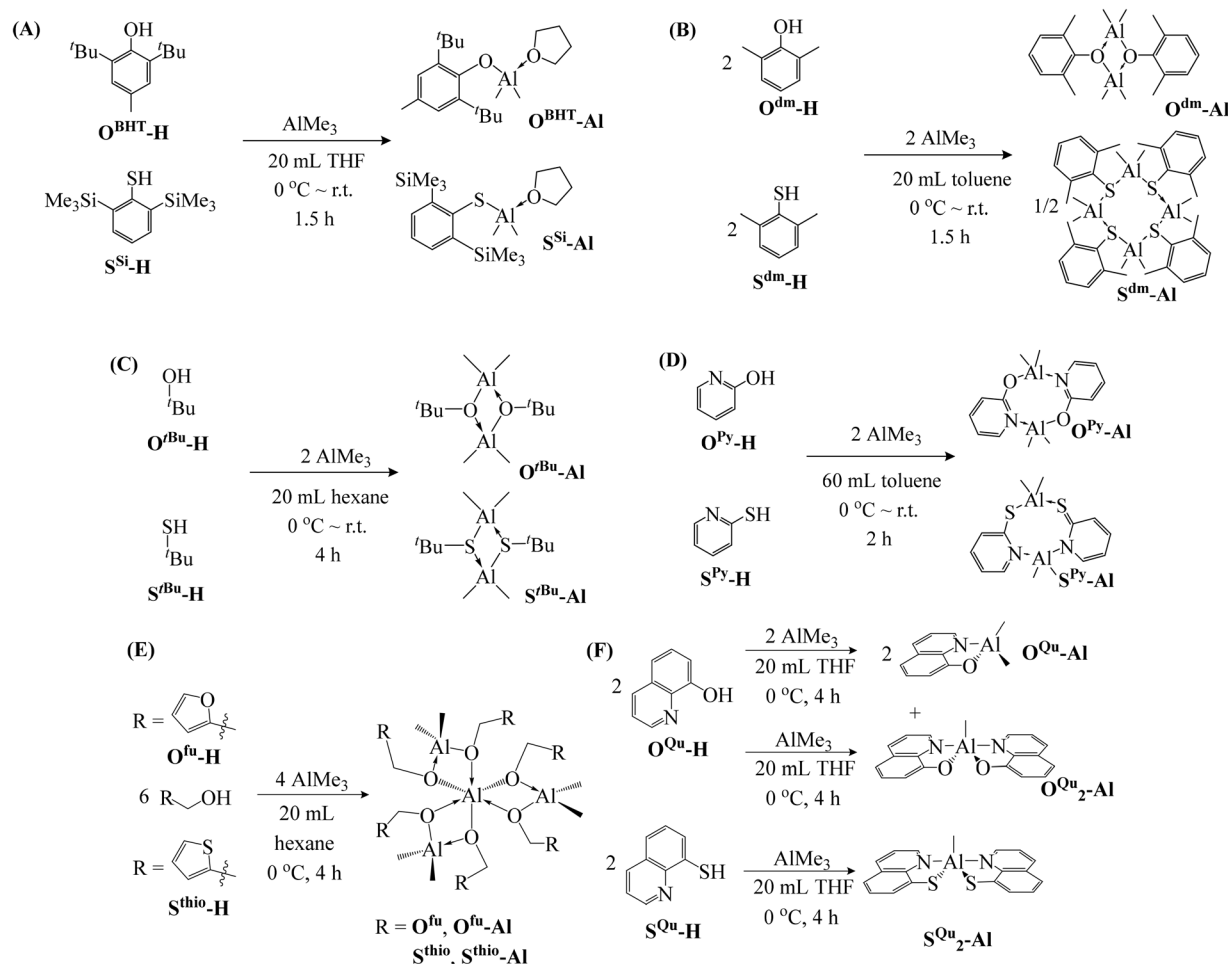


Fig. 3 Molecular structure of  $S^{Py}$ -Al depicted as ellipsoids at 30% probability (all hydrogen atoms are omitted for clarity).



Scheme 2 Synthesis of Al complexes bearing (A) 2,6-di-*tert*-butyl-4-methylphenolate ( $O^{BHT}$ ) and 2,6-bis(trimethylsilyl)benzenethiolate ( $S^{Si}$ ); (B) 2,6-di-methylphenolate ( $O^{dm}$ ) and 2,6-dimethylbenzenethiolate ( $S^{dm}$ ); (C) 2-methylpropan-2-olate ( $O^{tBu}$ ) and 2-methylpropan-2-thiolate ( $S^{tBu}$ ); (D) pyridin-2-olate ( $O^{Py}$ ) and pyridin-2-thiolate ( $S^{Py}$ ); (E) furan-2-ylmethanolate ( $O^{fu}$ ) and thiophen-2-ylmethanolate ( $S^{thio}$ ); (F) quinolin-8-olate ( $O^{Qu}$ ) and quinoline-8-thiolate ( $S^{Qu}$ ).

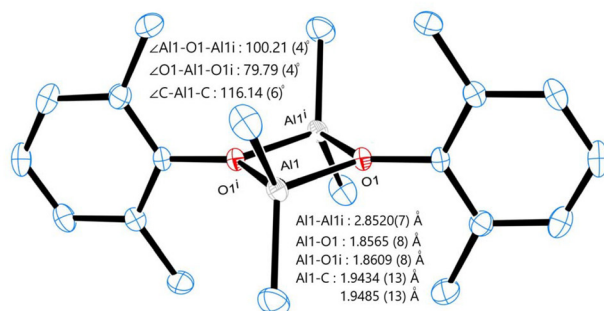
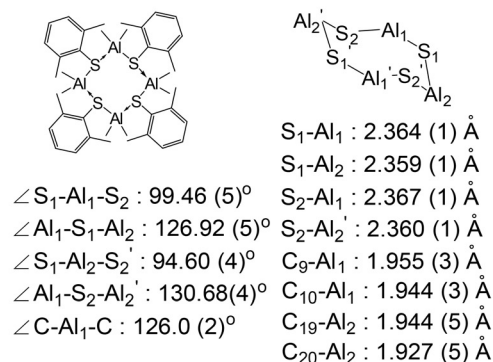
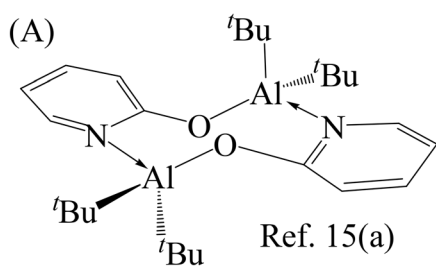
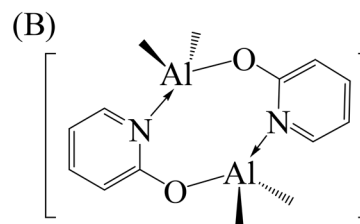
(A)  $\text{O}^{\text{dm}}\text{-Al}$ (B)  $\text{S}^{\text{dm}}\text{-Al}$ 

Fig. 2 Molecular structure of (A)  $\text{O}^{\text{dm}}\text{-Al}$  depicted as ellipsoids at 50% probability (all hydrogen atoms are omitted for clarity) and (B)  $\text{S}^{\text{dm}}\text{-Al}$  with selected bond angles and bond lengths.



Ref. 15(a)



Ref. 15(b)

Fig. 4 (A) Molecular structure of di-tert-butyl Al pyridine-2-olate and (B) proposed structure of  $\text{OPy-Al}$ .

## Results and discussion

### Synthesis and characterization of Al complexes

2,6-Bis(trimethylsilyl)benzenethiol<sup>13</sup> ( $\text{S}^{\text{Si}}\text{-H}$ ) was synthesized according to a reported procedure. Ligands, including  $\text{S}^{\text{Si}}\text{-H}$ ,

$\text{O}^{\text{BHT}}\text{-H}$ ,  $\text{S}^{\text{dm}}\text{-H}$ ,  $\text{O}^{\text{dm}}\text{-H}$ ,  $\text{S}^{\text{tBu}}\text{-H}$ ,  $\text{O}^{\text{tBu}}\text{-H}$ ,  $\text{S}^{\text{Py}}\text{-H}$ ,  $\text{O}^{\text{Py}}\text{-H}$ , and  $\text{O}^{\text{Qu}}\text{-H}$ , were reacted with trimethylaluminum ( $\text{AlMe}_3$ ) in a 1 : 1 ratio to afford dimethyl Al complexes, as confirmed by nuclear

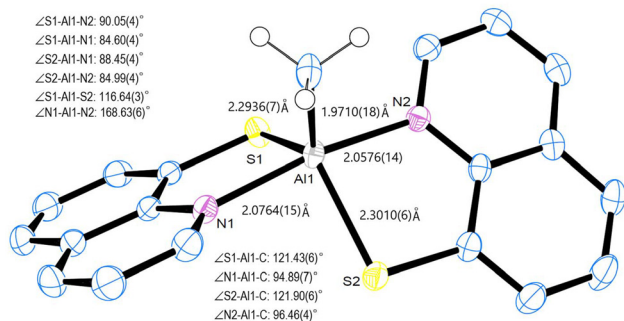


Fig. 5 Molecular structure of  $\text{S}^{\text{Qu}}\text{-Al}$  depicted as ellipsoids at 30% probability (all hydrogen atoms are omitted for clarity).

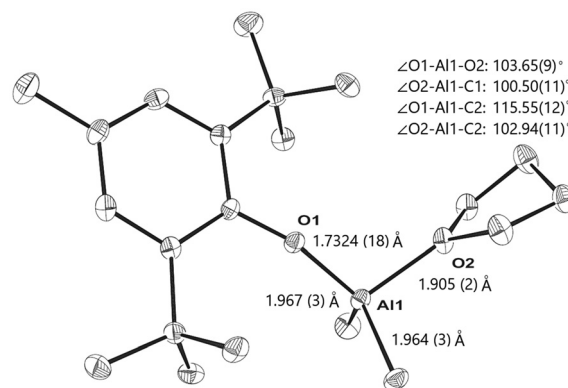


Fig. 6 Molecular structure of  $\text{O}^{\text{BHT}}\text{-Al}$  depicted as ellipsoids at 30% probability (all hydrogen atoms are omitted for clarity).

Table 1 CL polymerization performed using Al complexes as catalysts<sup>a</sup>

Entry	[CL]:[Al]:[BnOH] 100:x:2	Time (min)	Conv. <sup>b</sup> (%)	$M_n$ Cal <sup>b</sup>	$M_n$ NMR <sup>c</sup>	$M_n$ GPC <sup>d</sup>	$D^d$	$k_{obs} \times 10^3$ (error) min <sup>-1</sup>
1	<b>O<sup>BHT</sup>-Al</b> , x = 1	110	86	5000	3100	2300	1.04	19.5 (5)
2	<b>S<sup>Si</sup>-Al</b> , x = 1	35	92	5400	5900	9700	1.19	73.9 (43)
3	<b>O<sup>dm</sup>-Al</b> , x = 0.5	131	95	5500	5500	8500	1.17	22.8 (2)
4	<b>S<sup>dm</sup>-Al</b> , x = 0.25	20	95	5500	4800	7200	1.18	162.2 (99)
5	<b>O<sup>tBu</sup>-Al</b> , x = 0.5	60	94	5500	5300	6300	1.16	61.9 (18)
6	<b>S<sup>tBu</sup>-Al</b> , x = 0.5	16	92	5400	5800	6500	1.48	184.5 (63)
7	<b>O<sup>py</sup>-Al</b> , x = 0.5	1340	88	5100	5500	5500	1.11	1.6 (1)
8	<b>S<sup>py</sup>-Al</b> , x = 0.5	130	93	5400	5600	7700	1.23	21.0 (6)
9	<b>O<sup>fu</sup>-Al</b> , x = 0.33	270	92	5400	6200	4600	1.07	15.6 (7)
10	<b>S<sup>thio</sup>-Al</b> , x = 0.33	100	92	5400	4300	6000	1.09	35.0 (20)
11	<b>O<sup>Qu</sup>-Al</b> , x = 1	206	91	5300	5800	8900	1.27	13.3 (5)
12 <sup>e</sup>	<b>O<sup>Qu</sup><sub>2</sub>-Al</b> , x = 1	1900	91	10 400	12 800	9800	1.07	1.3 (1)
13 <sup>e</sup>	<b>S<sup>Qu</sup><sub>2</sub>-Al</b> , x = 1	103	87	10 100	12 100	19 500	1.04	21.7 (25)

<sup>a</sup> In general, the reaction was carried out in toluene with [CL] = 2 M, at 25 °C. <sup>b</sup> Calculated from the molecular weight of  $M_w(\text{CL}) \times [\text{CL}]_0/[\text{BnOH}]_0 \times \text{conversion yield} + M_w(\text{BnOH})$ . <sup>c</sup> Values of  $M_n$  NMR were obtained through <sup>1</sup>H NMR analysis that was calculated from the molecular mass of CL  $\times$  (the integration of the peak at 4.0 ppm/the integration of the peak at 7.3 ppm)  $\times$  5/2 +  $M_w(\text{BnOH})$ . <sup>d</sup> Values of  $M_n$  GPC were obtained from the number-average molecular weight (obtained through gel permeation chromatography) times 0.56 for PCL. <sup>e</sup> [CL]:[Al]:[BnOH] = 100:1:1, [CL] = 2 M at 50 °C.

magnetic resonance (NMR) spectroscopy. However, **O<sup>Qu</sup>-Al** is not stable; during the purification process, about half of **O<sup>Qu</sup>-Al** decomposes to form **O<sup>Qu</sup><sub>2</sub>-Al**. In addition, the dimethyl Al complex synthesized using **S<sup>Qu</sup>-H** as the ligand is extremely unstable—even in the initial reaction, half of the product is

**S<sup>Qu</sup><sub>2</sub>-Al** earlier on. After the purification, it is completely converted to **S<sup>Qu</sup><sub>2</sub>-Al**. Monomethyl Al complexes (**O<sup>Qu</sup><sub>2</sub>-Al** and **S<sup>Qu</sup><sub>2</sub>-Al**, Scheme 2F) were synthesized with a 2:1 ligand-to-AlMe<sub>3</sub> ratio, and the ligands were quinolin-8-ol (**O<sup>Qu</sup>-H**) and quinoline-8-thiol (**S<sup>Qu</sup>-H**), respectively. **O<sup>fu</sup>-Al** and **S<sup>thio</sup>-Al** were

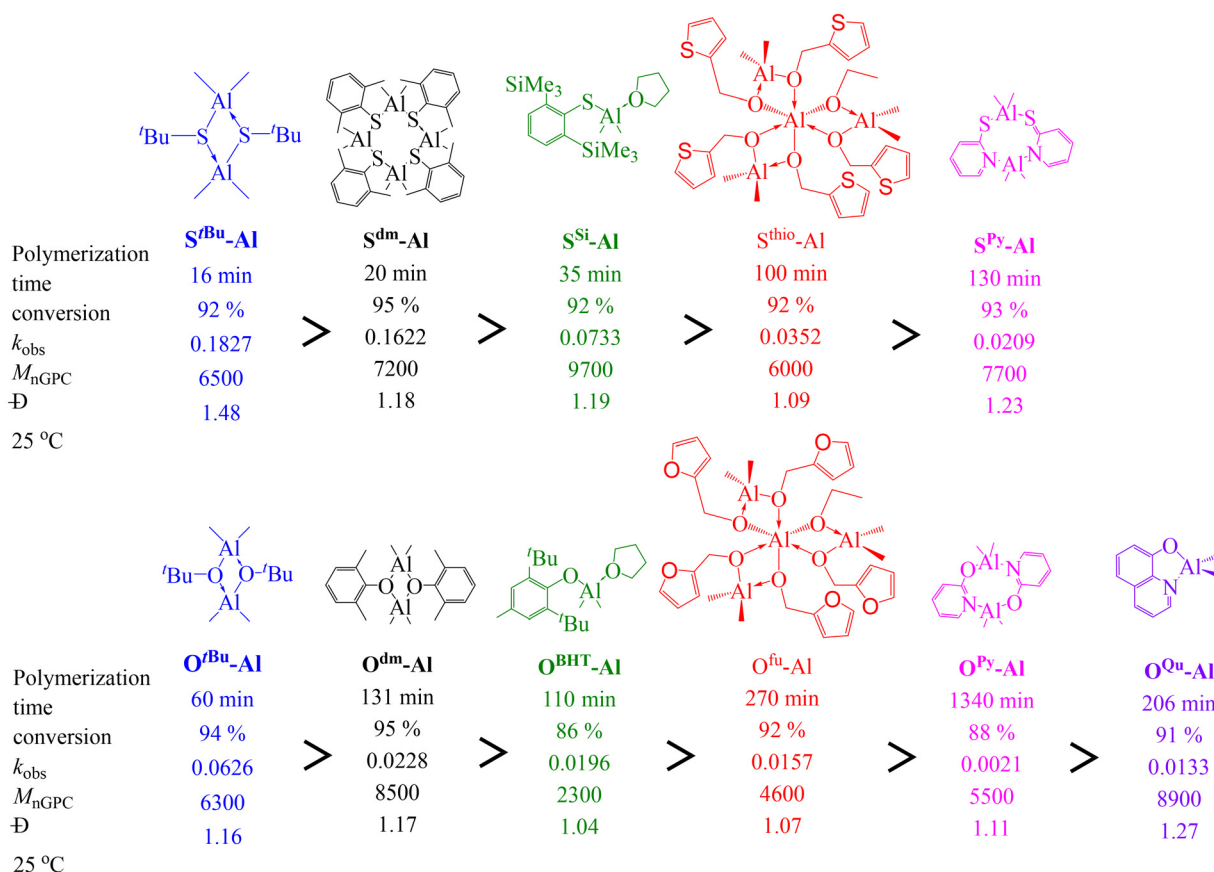


Fig. 7 Outcomes of CL polymerization performed using various Al complexes as catalysts.



**Table 2** CL polymerization by using  $\text{S}^{\text{dm}}\text{-Al}$  and  $\text{O}^{\text{dm}}\text{-Al}$  as catalysts and BnOH as an initiator

Entry	[CL]:[Al catalyst]:[BnOH]	Time (min)	Conv. <sup>a</sup> (%)	$M_n$ Cal <sup>b</sup>	$M_n$ NMR <sup>c</sup>	$M_n$ GPC <sup>d</sup>	$D^d$
1	100 : 1 : 2; $\text{S}^{\text{dm}}\text{-Al}$	34	95	5500	4000	4300	1.09
2	200 : 1 : 2 (entry 1 + 100 CL)	95	90	10 400	9100	9800	1.07
3	300 : 1 : 2 (entry 2 + 100 CL)	270	91	15 500	13 100	13 300	1.37
4	400 : 1 : 2 (entry 3 + 100 CL)	650	87	28 000	18 800	19 300	1.27
5	100 : 1 : 2; $\text{O}^{\text{dm}}\text{-Al}$	121	92	5400	5000	4800	1.16
6	200 : 1 : 2 (entry 5 + 100 CL)	340	90	10 400	10 600	10 100	1.11
7	300 : 1 : 2 (entry 6 + 100 CL)	639	84	14 500	14 600	14 400	1.11
8	400 : 1 : 2 (entry 7 + 100 CL)	1426	90	20 600	22 500	20 000	1.26

Reaction conditions: toluene (5 mL), [Al catalyst] = 0.02 M, 1.14 g CL for every loading, at 25 °C. <sup>a</sup> Data were obtained through <sup>1</sup>H NMR analysis.

<sup>b</sup> Calculated from the molecular weight of  $M_w(\text{CL}) \times [\text{CL}]_0/[\text{BnOH}]_0 \times \text{conversion yield} + M_w(\text{BnOH})$ . <sup>c</sup>  $M_n$  NMR was calculated from the molecular weight of CL  $\times$  (the integration of the peak at 4.0 ppm/the integration of the peak at 7.3 ppm)  $\times$  5/2 +  $M_w(\text{BnOH})$ . <sup>d</sup> Values of  $M_n$  GPC were obtained from the number-average molecular weight (obtained through gel permeation chromatography) times 0.56 for PCL.

synthesized by using a 3 : 2 ligand-to-AlMe<sub>3</sub> ratio. The crystal structure of  $\text{O}^{\text{BHT}}\text{-Al}$  exhibits a tetrahedral geometry; therefore, the  $\text{S}^{\text{Si}}\text{-Al}$  complex, composed of  $\text{S}^{\text{Si}}$ , THF, and two methyl groups, is also expected to possess a similar tetrahedral geometry, as shown in Scheme 2A. Because  $\text{S}^{\text{tBu}}\text{-Al}$  was reported to possess a dinuclear structure bridged by *tert*-butyl thiolate,  $\text{O}^{\text{tBu}}\text{-Al}$  was reasonably inferred to be a dinuclear structure (Scheme 2C).  $\text{O}^{\text{fu}}\text{-Al}$  and  $\text{S}^{\text{thio}}\text{-Al}$  were reported to be tetranuclear Al complexes (Scheme 2E). From the <sup>1</sup>H NMR spectrum of  $\text{O}^{\text{Qu}}\text{-Al}$ , only quinolin-8-olate and the methyl group on the Al atom (1 : 2 ratio) were observed, and a four-coordinated mononuclear Al structure (Scheme 2F) was proposed.

Al complexes, including  $\text{O}^{\text{dm}}\text{-Al}$ ,  $\text{S}^{\text{Py}}\text{-Al}$ ,  $\text{S}^{\text{Qu}}_2\text{-Al}$ , and  $\text{O}^{\text{BHT}}\text{-Al}$ , were crystallized from a highly concentrated toluene solution in an NMR tube at −25 °C. Single-crystal X-ray diffraction of dinuclear  $\text{O}^{\text{dm}}\text{-Al}$  (Cambridge Crystallographic Data Centre [CCDC] 2386783) revealed Al centers with a distorted tetrahedral geometry ( $\tau_4 = 0.92$ ),<sup>14</sup> coordinated by two oxygen atoms from the  $\text{O}^{\text{dm}}$  ligand and two methyl groups [Fig. 2(A)]. In comparison,  $\text{S}^{\text{dm}}\text{-Al}$  exhibited a slightly more distorted geometry [ $\tau_4 = 0.89$ , Fig. 2(B)]. The C–Al–C angle (116.14°) in  $\text{O}^{\text{dm}}\text{-Al}$  is smaller than the corresponding angles in  $\text{S}^{\text{dm}}\text{-Al}$  (126.0° and 126.3°), while the O–Al–C angles (113.07–115.48°) in  $\text{O}^{\text{dm}}\text{-Al}$  are larger than the S–Al–C angles (103.5–108.9°) in  $\text{S}^{\text{dm}}\text{-Al}$ .<sup>15</sup> These discrepancies can be attributed to the smaller atomic radius of oxygen compared to sulfur, which results in shorter O–Al bonds in  $\text{O}^{\text{dm}}\text{-Al}$  than the S–Al bonds in  $\text{S}^{\text{dm}}\text{-Al}$ . The shorter Al–O bonds bring the two methyl groups on the aluminum atom, and the methyl substituents on the phenyl rings, closer together, thereby increasing steric repulsion. This increased repulsion forces the two methyl groups on the Al center closer to each other, necessitating larger O–Al–C bond angles to reduce the steric strain and maintain structural stability.

The crystal structure of dinuclear  $\text{S}^{\text{Py}}\text{-Al}$  (CCDC 2386781, Fig. 3) revealed the presence of two distinct aluminum centers. One Al atom [Al(1)] reveals a geometry ( $\tau_4 = 0.78$ ) between trigonal pyramidal and seesaw shape with two sulfur atoms from the  $\text{S}^{\text{Py}}$  ligand and two methyl groups. The other Al atom [Al(2)] exhibits a distorted tetrahedral geometry ( $\tau_4 = 0.88$ ) with two nitrogen atoms from the  $\text{S}^{\text{Py}}$  ligand and two methyl groups. Notably,

the head-to-head arrangement of the  $\text{S}^{\text{Py}}\text{-Al}$  differs significantly from the head-to-tail structure observed in  $\text{O}^{\text{Py}}\text{-Al}$ <sup>16</sup> (Fig. 4).

The crystal structure of dinuclear  $\text{S}^{\text{Qu}}\text{-Al}$  (CCDC 2386782; Fig. 5) revealed that the Al atoms possessed a distorted trigonal bipyramidal geometry ( $\tau_5 = 0.78$ ). The axial N1–Al1–N2 bond angle is compressed, averaging 168.63(6)°, while the equatorial bond angles of S1–Al1–S2, S1–Al1–C, and S(2)–Al1–C are 116.64(3)°, 121.43(6)°, and 121.90(6)°, respectively. Additionally, the bond distances between the Al1 atom and S1, S2, N1, N2 and C are 2.2936(7), 2.3010(6), 2.0764(15), 2.0576(14) and 1.9710(18) Å, respectively.

The crystal structure of dinuclear  $\text{O}^{\text{BHT}}\text{-Al}$  (CCDC 2468931; Fig. 6) revealed that the Al atoms possessed a tetrahedral geometry ( $\tau_4 = 0.99$ ) coordinated by two oxygen atoms from the BHT ligand and THF and two methyl groups. Additionally, the bond distances between the Al1 atom and O1, O2, C1, and C2 are 1.7324(18), 1.905(2), 1.964(3), and 1.967(3) Å, respectively.

## CL polymerization

Table 1 and Fig. 7 summarize the catalytic performance of the Al complexes in the ROP of CL in toluene. Benzyl alcohol

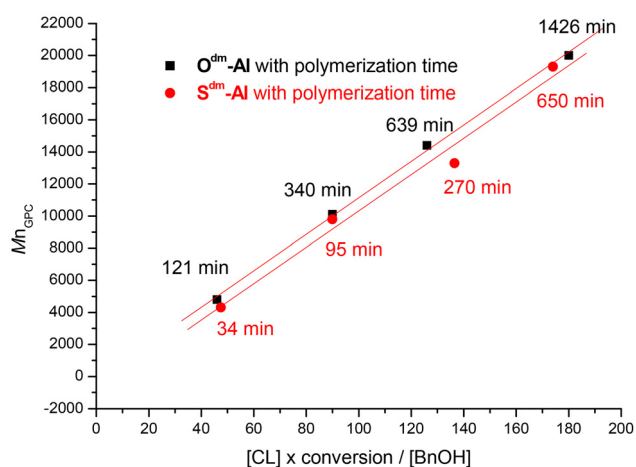


**Fig. 8** Linear plot of  $M_n$  GPC vs.  $[\text{CL}]_0 \times \text{conv.}/[\text{BnOH}]$  for  $\text{O}^{\text{dm}}\text{-Al}$  (black dot, entries 1–4 of Table 2) and  $\text{S}^{\text{dm}}\text{-Al}$  (red dot, entries 5–8 Table 2).

(BnOH) was employed as the initiator, as the methyl groups on the Al centers are inefficient initiators of the polymerization reaction.<sup>17</sup> Among the tested catalysts,  $\text{S}^{\text{Si}}\text{-Al}$  exhibited significantly higher catalytic activity ( $[\text{CL}]:[\text{S}^{\text{Si}}\text{-Al}]:[\text{BnOH}] = 100:1:2$ ;  $[\text{CL}] = 2 \text{ M}$ ; conv. = 92% at 25 °C after 35 min;  $k_{\text{obs}} = 0.0733 \text{ min}^{-1}$ ; entry 2 in Table 1) compared to  $\text{O}^{\text{BHT}}\text{-Al}$  ( $k_{\text{obs}} = 0.0196 \text{ min}^{-1}$ ; entry 1 in Table 1) corresponding to a 3.7-fold

increase in the observed rate constant. Other types of sulfur-containing Al complexes also demonstrated superior polymerization rates compared to their oxygen-containing analogues: 7.1-fold ( $\text{S}^{\text{dm}}\text{-Al}$  vs.  $\text{O}^{\text{dm}}\text{-Al}$ ), 2.9-fold ( $\text{S}^{\text{tBu}}\text{-Al}$  vs.  $\text{O}^{\text{tBu}}\text{-Al}$ ), 10.0-fold ( $\text{S}^{\text{Py}}\text{-Al}$  vs.  $\text{O}^{\text{Py}}\text{-Al}$ ), 2.2-fold ( $\text{S}^{\text{thio}}\text{-Al}$  vs.  $\text{O}^{\text{fu}}\text{-Al}$ ), and 16.4-fold ( $\text{S}^{\text{Qu}_2}\text{-Al}$  vs.  $\text{O}^{\text{Qu}_2}\text{-Al}$ ) increase. Among all catalysts evaluated,  $\text{S}^{\text{tBu}}\text{-Al}$  exhibited the highest catalytic activity; however, it

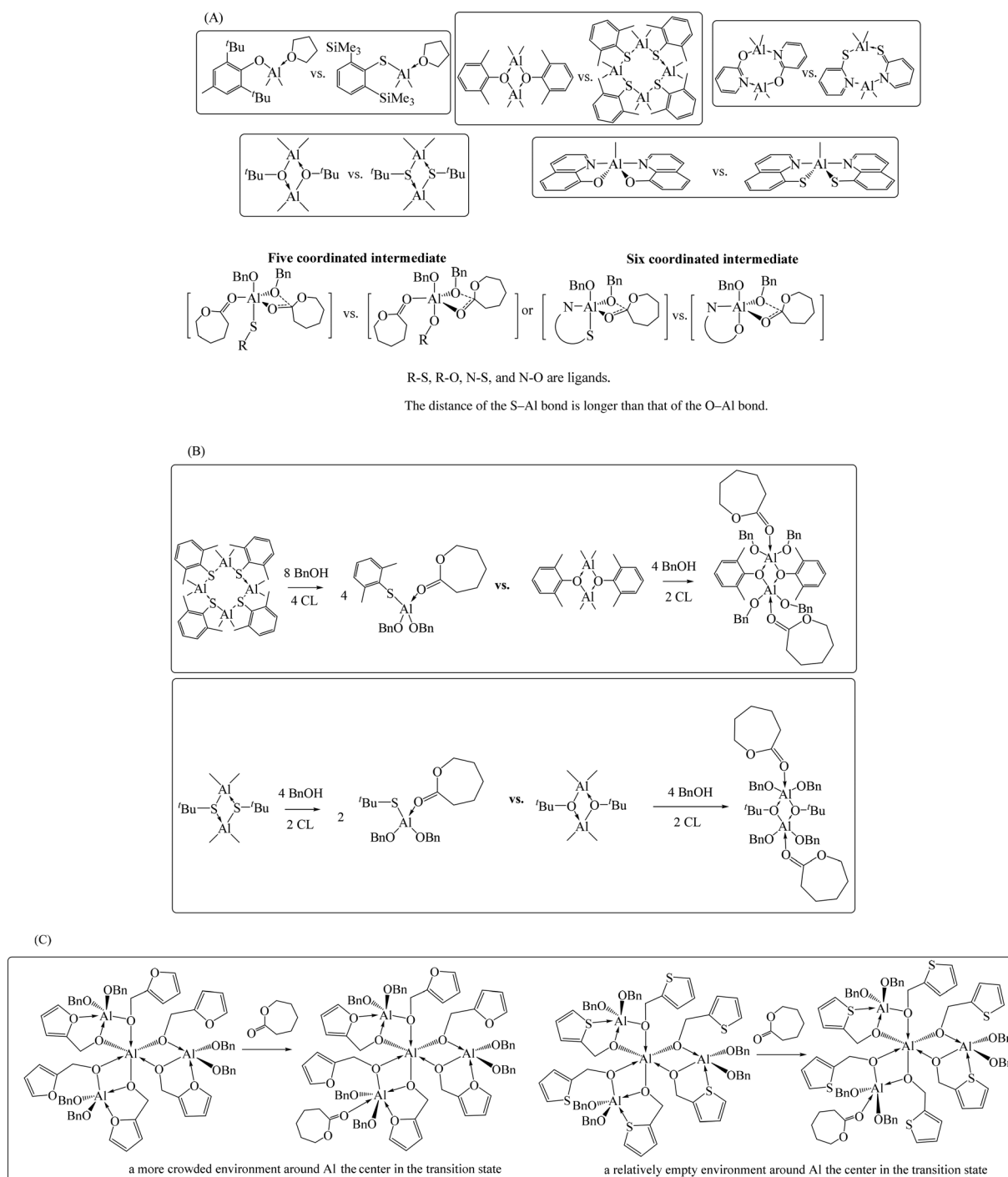


**Fig. 9** Reasons for the higher catalytic activity of Al complexes bearing sulfur-containing ligands compared to those of oxygen-containing ligands: (A) Ligand repulsion, (B) bridging atom dissociation, and (C) chelating atom dissociation.

displayed poor control over polymerization, as indicated by a high dispersity ( $D = 1.48$ ). Furthermore, the Al complexes bearing bidentate ligands such as  $\text{O}^{\text{Py}}$ ,  $\text{S}^{\text{Py}}$ ,  $\text{O}^{\text{fu}}$ ,  $\text{S}^{\text{thio}}$ ,  $\text{O}^{\text{Qu}}$ , and  $\text{S}^{\text{Qu}}$  exhibited lower catalytic activity than those with monodentate ligands. Notably, the Al complexes bearing quinoline type ligands revealed the lowest catalytic performance (especially  $\text{O}^{\text{Qu}}_2\text{-Al}$  and  $\text{S}^{\text{Qu}}_2\text{-Al}$  are inactive at 25 °C). This reduced activity is attributed to the rigid structure of the quinoline ligands, which hinders quinoline dissociation from the Al center. In addition, bis-ligated complexes such as  $\text{O}^{\text{Qu}}_2\text{-Al}$  and  $\text{S}^{\text{Qu}}_2\text{-Al}$  form sterically congested, “crowned” aluminum centers that impede effective coordination with the CL monomer. Surveying all the GPC data (Table 1) of the produced PCL, it can be observed that the PCLs generated using  $\text{S}^{\text{Si}}\text{-Al}$  (entry 2),  $\text{O}^{\text{dm}}\text{-Al}$  (entry 3),  $\text{S}^{\text{dm}}\text{-Al}$  (entry 4),  $\text{O}^{\text{Qu}}\text{-Al}$  (entry 11),  $\text{O}^{\text{Qu}}_2\text{-Al}$  (entry 12), and  $\text{S}^{\text{Qu}}_2\text{-Al}$  (entry 13) exhibited a large difference between their  $M_{\text{n GPC}}$  and  $M_{\text{n NMR}}$  values (greater than 3000 g mol<sup>-1</sup>). These discrepancies were attributed to the transesterification when using these catalysts. Another possible reason is that the initiation is slower than the propagation, leading to poorer catalyst controllability, and thus the  $M_{\text{n GPC}}$  of the resulting polymer becomes larger than the  $M_{\text{n NMR}}$ .

Since  $\text{S}^{\text{dm}}\text{-Al}$  exhibited the second highest catalytic activity and produced PCL with a narrow  $D$  value (1.18), the polymerization controllability of  $\text{S}^{\text{dm}}\text{-Al}$  and  $\text{O}^{\text{dm}}\text{-Al}$  in CL ROP was further investigated and the results are listed in Table 2. For each catalyst, two equivalents of BnOH were combined with 100 equivalents of CL in 5 mL of toluene, using 0.25 equivalents of  $\text{S}^{\text{dm}}\text{-Al}$  or 0.5 equivalent of  $\text{O}^{\text{dm}}\text{-Al}$ . After achieving >90% conversion, an additional 100 equivalents of CL monomers were added to the reaction mixture. This process was repeated until the solution became too viscous to stir, which occurred after three additions of CL, resulting in a final [CL]:[BnOH] ratio of 400:2 (Table 2). The linear correlation between the number-average molecular weight determined by GPC ( $M_{\text{n GPC}}$ ) and  $([\text{CL}]_0 \times \text{conv.})/[\text{BnOH}]$  (Table 2) shown in Fig. 8 demonstrates that both  $\text{S}^{\text{dm}}\text{-Al}$  and  $\text{O}^{\text{dm}}\text{-Al}$  catalyzed highly controlled polymerizations with narrow  $D$  values (1.07–1.37 for  $\text{S}^{\text{dm}}\text{-Al}$  and 1.11–1.26 for  $\text{O}^{\text{dm}}\text{-Al}$ ). These results indicate living characteristics of  $\text{S}^{\text{dm}}\text{-Al}$  and  $\text{O}^{\text{dm}}\text{-Al}$  in CL ROP. Nevertheless, the catalytic activity of  $\text{S}^{\text{dm}}\text{-Al}$  consistently outperformed that of  $\text{O}^{\text{dm}}\text{-Al}$  throughout the study.

The experimental results above clearly demonstrate that aluminum complexes bearing sulfur-containing ligands exhibit higher catalytic activity than their oxygen-containing counterparts. This enhanced activity is presumably due to two main factors. First, the S–Al bond is longer than the O–Al bond. Our previous studies<sup>11,18</sup> supported that the longer S–Al bond reduces the repulsion in the crowded intermediate (Fig. 9A), thereby lowering the activation energy compared to complexes with shorter Al–O bonds. Second, sulfur atoms in chelating ligands can more readily dissociate from the aluminum center than oxygen atoms.<sup>8d,l</sup> This dynamic dissociation creates more open coordination space around the aluminum, facilitating the effective coordination of the CL monomer and enhancing catalytic efficiency (Fig. 9B). The reason why  $\text{S}^{\text{thio}}\text{-Al}$

exhibited higher catalytic activity than  $\text{O}^{\text{fu}}\text{-Al}$  is that the bond between the sulfur atom on the thiophenyl group ( $\text{S}^{\text{thio}}\text{-Al}$ ) and the Al atom is weaker. When CL coordinates to the Al center, the sulfur atom on the thiophenyl group can dissociate first, creating more space to facilitate the CL coordination. In contrast, the bond between the oxygen atom on the furanyl group ( $\text{O}^{\text{fu}}\text{-Al}$ ) and the Al atom is stronger, so the oxygen does not dissociate when CL attempts to coordinate to the Al center. As a result, a more crowded six-coordinate Al center in  $\text{O}^{\text{fu}}\text{-Al}$  system must form, which in turn reduces the catalytic activity. A similar conclusion was also reported in previous studies<sup>8d</sup> on ferrocene-based thioether phenolate Al complexes for CL polymerization.

## Conclusions

We synthesized and evaluated the catalytic activity in the CL ROP of a series of Al complexes bearing alcoholate, alkyl thiolate, phenolate, and aryl thiolate groups. The polymerization results demonstrated that Al complexes bearing sulfur-containing ligands exhibited significantly higher catalytic activity (2.2 to 16.4 fold) compared to their oxygen-containing counterparts. Among them,  $\text{S}^{\text{fbu}}\text{-Al}$  exhibited the highest catalytic activity; however, it displayed poor control over the polymerization process. Conversely, Al complexes bearing quinoline-type ligands exhibited the lowest catalytic activity. Notably,  $\text{S}^{\text{dm}}\text{-Al}$  exhibited the second highest catalytic activity and achieved well-controlled CL polymerization. This study offers valuable insights for researchers in the field of ring-opening polymerization: the incorporation of sulfur atoms into ligand structures can substantially enhance the catalytic efficiency of aluminum complexes.

## Experimental section

Standard Schlenk techniques and an N<sub>2</sub>-filled glovebox were used throughout the compounds' isolation and handling. Solvents,  $\epsilon$ -caprolactone, and deuterated solvents were purified before use.  $\epsilon$ -Caprolactone was purified by distillation with magnesium sulfate anhydrous. The organic solvents, including toluene, THF, and hexane, were purified by distillation in the presence of sodium and benzophenone. Deuterated chloroform was purified by distillation in the presence of calcium hydride. Deuterated chloroform, furfuranol, thiophen-2-ylmethanol,  $\epsilon$ -caprolactone, benzyl alcohol, *N,N,N,N*-tetramethylethylenediamine, trimethylaluminum (2 M in toluene), chlorotrimethylsilane, 2,6-di-*tert*-butyl-4-methylphenol, 2,6-dimethylphenol, 2,6-dimethylthiophenol, *tert*-butanol, *tert*-butylthiol, 8-hydroxyquinoline, quinoline-8-thiol, pyridin-2-ol and 2-mercaptopyridine were purchased from Sigma-Aldrich. Thiophenol was purchased from Showa. *n*-Butyl lithium (2.5 M in *n*-hexane) was purchased from Chemetall. <sup>1</sup>H spectra were recorded on a Varian Gemini2000-200 (200 MHz) and JEOL (400 MHz) spectrometers and <sup>13</sup>C NMR spectra were recorded



on a JEOL (100 MHz for  $^{13}\text{C}$ ) spectrometer with chemical shifts given in ppm from the internal TMS or center line of  $\text{CDCl}_3$ . Microanalyses were performed using a Heraeus CHN-O-RAPID instrument. GPC measurements were performed on a Jasco PU-2080 PLUS HPLC pump system equipped with a differential Jasco RI-2031 PLUS refractive index detector using THF (HPLC grade) as an eluent (flow rate  $1.0\text{ mL min}^{-1}$ , at  $40\text{ }^\circ\text{C}$ ). The chromatographic column was JORDI Gel DVB  $10^3\text{ \AA}$ , and the calibration curve was made by primary polystyrene standards to calculate  $M_{\text{n GPC}}$ . All single X-ray diffraction data were accumulated using Rigaku Oxford Diffraction single crystal X-ray diffractometers with Mo  $\text{K}\alpha$  radiation ( $\lambda = 0.71073\text{ \AA}$ ). The data were collected using the CrysAlisPro 1.171.41.56a program. Cell refinement and data reduction were performed using the CrysAlisPro 1.171.41.56a program. The structure was determined using the Olex2/ShelXL program refined using full-matrix least squares. All non-hydrogen atoms were refined anisotropically, whereas hydrogen atoms were placed at calculated positions and included in the final stage of refinement with fixed parameters.  $\text{S}^{\text{Si}}\text{-H}$ ,<sup>13</sup>  $\text{O}^{\text{dm}}\text{-Al}$ ,<sup>19</sup>  $\text{S}^{\text{dm}}\text{-Al}$ ,<sup>20</sup>  $\text{S}^{\text{tBu}}\text{-Al}$ ,<sup>21</sup>  $\text{O}^{\text{fu}}\text{-Al}$ ,<sup>22</sup>  $\text{S}^{\text{thio}}\text{-Al}$ ,<sup>22</sup>  $\text{O}^{\text{Py}}\text{-Al}$ ,<sup>16</sup> and  $\text{S}^{\text{Py}}\text{-Al}$ <sup>23</sup> were prepared following literature procedures.

### Synthesis of $\text{O}^{\text{BHT}}\text{-Al}$

A mixture of butylated hydroxytoluene ( $\text{O}^{\text{BHT}}\text{-H}$ , 1.10 g, 5.0 mmol) and  $\text{AlMe}_3$  (2.8 mL, 2.0 M, 5.6 mmol) in THF (20 mL) was stirred at  $0\text{ }^\circ\text{C}$  for 1.5 h. Volatile materials were removed under vacuum to give a white powder, and then hexane (50 mL) was transferred to make a suspension. The white powder was obtained after filtering. Yield: 1.46 g (84%).  $^1\text{H}$  NMR ( $\text{CDCl}_3$ , 200 MHz)  $\delta$  7.00 (s, 2H, *o*- $\text{CH}_3\text{Ph-H}$ ), 4.20 (t, 4H,  $\text{CH}_2\text{CH}_2\text{O}$ ), 2.25 (s, 3H,  $\text{PhCH}_3$ ), 2.07 (t, 4H,  $\text{CH}_2\text{CH}_2\text{O}$ ), 1.39 (s, 18H,  $\text{C}(\text{CH}_3)_3$ ),  $-0.68$  (s, 6H,  $(\text{Al}(\text{CH}_3)_2)$ ).  $^{13}\text{C}$ -NMR (100 MHz,  $\text{CDCl}_3$ )  $\delta$  154.75 ( $\text{C-O}$  of ArO), 138.22 ( $\text{C}$  of *o*-ArO), 125.59 ( $\text{C}$  of *m*-ArO), 124.67 ( $\text{C}$  of *p*-ArO), 71.19 ( $\text{CH}_2\text{CH}_2\text{O}$ ), 34.60 ( $\text{PhC}(\text{CH}_3)_3$ ), 30.59 ( $\text{PhC}(\text{CH}_3)_3$ ), 24.92 ( $\text{CH}_2\text{CH}_2\text{O}$ ), 21.03 ( $\text{PhCH}_3$ ),  $-7.05$  ( $\text{Al}(\text{CH}_3)_2$ ). Anal. calc. (found) for  $\text{C}_{21}\text{H}_{37}\text{AlO}_2$ : C 72.37 (71.93), H 10.70 (10.90).

### Synthesis of $\text{S}^{\text{Si}}\text{-Al}$

$\text{S}^{\text{Si}}\text{-Al}$  was prepared according to the same procedure described for  $\text{O}^{\text{BHT}}\text{-Al}$ , except that  $\text{S}^{\text{Si}}\text{-H}$  was used instead of  $\text{O}^{\text{BHT}}\text{-H}$ . Volatile materials were removed under vacuum to give a colorless oil. Yield: 1.88 g (98%).  $^1\text{H}$  NMR ( $\text{CDCl}_3$ , 200 MHz)  $\delta$  7.48 (d, 2H,  $J = 8\text{ Hz}$ , *m*- $\text{PhS-H}$ ), 7.20 (t, 1H,  $J = 8\text{ Hz}$ , *p*- $\text{PhS-H}$ ), 3.96 (t, 4H,  $\text{CH}_2\text{CH}_2\text{O}$ ), 1.99 (t, 4H,  $\text{CH}_2\text{CH}_2\text{O}$ ), 1.39 (s, 18H,  $\text{Si}(\text{CH}_3)_3$ ),  $-0.92$  (s, 6H,  $(\text{Al}(\text{CH}_3)_2)$ ).  $^{13}\text{C}$ -NMR (100 MHz,  $\text{CDCl}_3$ )  $\delta$  143.35 ( $\text{C-S}$  of ArS), 136.12 ( $\text{C}$  of *m*-ArS), 125.63 ( $\text{C}$  of *o*-ArS), 123.57 ( $\text{C}$  of *p*-ArS), 69.90 ( $\text{CH}_2\text{CH}_2\text{O}$ ), 25.30 ( $\text{CH}_2\text{CH}_2\text{O}$ ), 0.29 ( $\text{Si}(\text{CH}_3)_3$ ),  $-9.72$  ( $\text{Al}(\text{CH}_3)_2$ ). Anal. calc. (found) for  $\text{C}_{18}\text{H}_{35}\text{AlOSSi}_2$ : C 56.49 (56.40), H 9.22 (9.48).

### Synthesis of $\text{O}^{\text{tBu}}\text{-Al}$

A mixture of *tert*-butanol (0.37 g, 5.0 mmol) and  $\text{AlMe}_3$  (2.8 mL, 2.0 M, 5.6 mmol) in hexane (20 mL) was stirred at  $0\text{ }^\circ\text{C}$  for 3.0 h. Volatile materials were removed under vacuum

to give a colorless oil. Yield: 1.30 g (99%).  $^1\text{H}$  NMR ( $\text{CDCl}_3$ , 200 MHz)  $\delta$  1.36 (s, 9H,  $\text{C}(\text{CH}_3)_3$ ),  $-0.73$  (s, 6H,  $(\text{Al}(\text{CH}_3)_2)$ ).  $^{13}\text{C}$ -NMR (100 MHz,  $\text{CDCl}_3$ )  $\delta$  74.40 ( $\text{C}(\text{CH}_3)_3$ ), 31.62 ( $\text{C}(\text{CH}_3)_3$ ),  $-6.93$  ( $\text{Al}(\text{CH}_3)_2$ ). Anal. calc. (found) for  $\text{C}_{12}\text{H}_{30}\text{Al}_2\text{O}_2$ : C 55.36 (55.05), H 11.62 (11.36).

### Synthesis of $\text{O}^{\text{Qu}}\text{-Al}$

A mixture of quinolin-8-ol ( $\text{O}^{\text{Qu}}\text{-H}$ , 1.45 g, 10.0 mmol) and  $\text{AlMe}_3$  (5.2 mL, 2.0 M, 10.4 mmol) in THF (50 mL) was stirred at  $0\text{ }^\circ\text{C}$  for 3 h. Volatile materials were removed under vacuum to give a white powder, and then the mixed solution [hexane (50 mL) + toluene (10 mL) at  $0\text{ }^\circ\text{C}$ ] was transferred to make a suspension and stirred for 1 h at  $0\text{ }^\circ\text{C}$ . The white powder was obtained after filtering. Yield: 1.50 g (74%).  $^1\text{H}$  NMR ( $\text{CDCl}_3$ , 400 MHz)  $\delta$  8.68 [dd, 1H,  $J = 4.0$  and  $1.3\text{ Hz}$ , 2-position ( $\text{N}=\text{C-H}$ )], 8.34 (dd, 1H,  $J = 8.0$  and  $1.4\text{ Hz}$ , 4-position), 7.61 (dd, 1H,  $J = 8.0$  and  $4.0\text{ Hz}$ , 3-position), 7.59 (t, 1H,  $J = 8.0\text{ Hz}$ , 6-position), 7.44 (d, 1H,  $J = 8.0\text{ Hz}$ , 5-position), 7.38 (d, 1H,  $J = 8.0\text{ Hz}$ , 7-position),  $-0.63$  (s, 6H,  $(\text{Al}(\text{CH}_3)_2)$ ).  $\text{O}^{\text{Qu}}\text{-Al}$  had a poor solubility in  $\text{CDCl}_3$  and it disintegrated in  $\text{d}_6\text{-DMSO}$ . Therefore, its  $^{13}\text{C}$  NMR spectrum could not be obtained. Anal. calc. (found) for  $\text{C}_{11}\text{H}_{12}\text{AlNO}$ : C 65.67 (65.25), H 6.01 (5.91), N 6.96 (6.77).

### Synthesis of $\text{O}^{\text{Qu}}_2\text{-Al}$

A mixture of quinolin-8-ol ( $\text{O}^{\text{Qu}}\text{-H}$ , 1.45 g, 10.0 mmol) and  $\text{AlMe}_3$  (2.6 mL, 2.0 M, 5.2 mmol) in THF (50 mL) was stirred at room temperature for 3 h. Volatile materials were removed under vacuum to give a white powder, and then hexane (50 mL) was transferred to make a suspension. The white powder was obtained after filtering. Yield: 1.30 g (79%).  $^1\text{H}$  NMR ( $\text{CDCl}_3$ , 400 MHz)  $\delta$  8.89 [dd, 2H,  $J = 5.0$  and  $1.2\text{ Hz}$ , 2-position ( $\text{N}=\text{C-H}$ )], 8.37 (dd, 2H,  $J = 8.3$  and  $1.3\text{ Hz}$ , 4-position), 7.64 [dd, 2H,  $J = 8.3$  and  $5.0\text{ Hz}$ , 3-position ( $\text{N}=\text{C-H}$ )], 7.50 (t, 2H,  $J = 7.8\text{ Hz}$ , 6-position), 7.19 (d, 2H,  $J = 7.8\text{ Hz}$ , 5-position), 7.05 (d, 2H,  $J = 7.8\text{ Hz}$ , 7-position),  $-0.71$  (s, 3H,  $(\text{AlCH}_3)$ ).  $^{13}\text{C}$ -NMR (100 MHz,  $\text{CDCl}_3$ )  $\delta$  157.99, 144.40, 140.11, 138.93, 130.62, 129.11, 122.20, 113.51, 112.58 ( $\text{C-quinolinyl}$  group), 1.17 ( $\text{AlCH}_3$ ). Anal. calc. (found) for  $\text{C}_{19}\text{H}_{15}\text{AlN}_2\text{O}_2$ : C 69.09 (68.94), H 4.58 (4.47), N 8.48 (8.28).

### Synthesis of $\text{S}^{\text{Qu}}_2\text{-Al}$

$\text{S}^{\text{Qu}}_2\text{-Al}$  was prepared according to the same procedure described for  $\text{O}^{\text{Qu}}_2\text{-Al}$ , except that  $\text{S}^{\text{Qu}}\text{-H}$  was used instead of  $\text{O}^{\text{Qu}}\text{-H}$ . Volatile materials were removed under vacuum to give a white powder, and then hexane (50 mL) was transferred to make a suspension. The white powder was obtained after filtering. Yield: 1.40 g (77%).  $^1\text{H}$  NMR ( $\text{CDCl}_3$ , 400 MHz)  $\delta$  8.95 [dd, 2H,  $J = 4.0$  and  $1.5\text{ Hz}$ , 2-position ( $\text{N}=\text{C-H}$ )], 8.38 (d, 2H,  $J = 8.0\text{ Hz}$ , 4-position), 7.86 (dd, 2H,  $J = 8.0$  and  $1.5\text{ Hz}$ , 5-position), 7.63 (dd, 2H,  $J = 8.0$  and  $4.8\text{ Hz}$ , 7-position), 7.49 (t, 2H,  $J = 8.0\text{ Hz}$ , 3-position), 7.45 (t, 2H,  $J = 8.0\text{ Hz}$ , 6-position),  $-0.37$  (s, 3H,  $(\text{AlCH}_3)$ ).  $^{13}\text{C}$ -NMR (100 MHz,  $\text{d}_6\text{-DMSO}$ )  $\delta$  147.16, 142.74, 141.49, 140.85, 130.08, 128.73, 128.54, 122.45, 121.61 ( $\text{C-quinolinyl}$  group),  $-0.99$  ( $\text{AlCH}_3$ ). Anal. calc. (found) for  $\text{C}_{19}\text{H}_{15}\text{AlN}_2\text{S}_2$ : C 62.96 (62.79), H 4.17 (4.05), N 7.73 (7.62).

## General procedures for the polymerization of $\epsilon$ -caprolactone

A typical polymerization procedure is exemplified by the synthesis shown in entry 1 (Table 1) using complex  $\mathbf{O}^{\text{BHT}}\text{-Al}$  as a catalyst. The polymerization conversion was analyzed by  $^1\text{H}$  NMR spectroscopic studies. Toluene (5.0 mL) was added to a mixture of complex  $\mathbf{O}^{\text{BHT}}\text{-Al}$  (0.017 g, 0.05 mmol),  $\text{BnOH}$  (0.10 mmol), and  $\epsilon$ -caprolactone (10 mmol) at room temperature. At indicated time intervals, 0.05 mL aliquots were removed, trapped with  $\text{CDCl}_3$  (1.0 mL), and analyzed by  $^1\text{H}$  NMR. After the solution was stirred for 110 min, the reaction was then quenched by adding acetic acid (2.0 mL), and the polymer precipitated as a white solid when pouring into  $n$ -hexane (50.0 mL). The isolated white solid was dissolved in  $\text{CH}_2\text{Cl}_2$  (20.0 mL), and water (20.0 mL) was used to wash the organic solution. Volatile materials were removed under vacuum to give a purified crystalline solid. Yield: 1.01 g (89%).

## Author contributions

T.-Y. L., Y.-C. L., and S.-Y. H. performed the experiments; T. B. H. performed additional edits and proof reading; R. K. prepared the graphical abstract. H.-C. T and S. D. performed NMR measurements; H.-Y. C. and C.-M. L. conceptualized the project and wrote and edited the manuscript. All authors have read and agreed to the published version of the manuscript.

## Conflicts of interest

The authors declare no conflict of interest.

## Data availability

The authors confirm that the data supporting the findings of this study are available within the article and its SI: polymer characterization data and details of the kinetic study. See DOI: <https://doi.org/10.1039/d5dt01410g>.

CCDC 2386781–2386783 and 2468931 contain the supplementary crystallographic data for this paper.<sup>24a–d</sup>

## Acknowledgements

This study was supported by the National Science and Technology Council of Taiwan (grant NSTC 113-2113-M-037-001, 111-2314-B-037-094-MY3, and 113-2113-M-037-009) and Kaohsiung Medical University “NSYSU-KMU JOINT RESEARCH PROJECT” (NSYSU-KMU-113-P24, KMU-DK109004, and KMU-TB114009). We thank the Center for Research Resources and Development at Kaohsiung Medical University for instrumentation and equipment support as well as for providing storage resources.

## References

- (a) Y. Mato, T. Isobe, H. Kanehiro, C. Ohtaka and T. Kaminuma, *Environ. Sci. Technol.*, 2001, **35**, 318–324; (b) C. M. Rochman, E. Hoh, B. T. Hentschel and S. Kaye, *Environ. Sci. Technol.*, 2013, **47**, 1646–1654; (c) C. M. Rochman, E. Hoh, T. Kurobe and S. J. Teh, *Sci. Rep.*, 2013, **3**, 3263; (d) D. S. Green, B. Boots, D. J. Blockley, C. Rocha and R. Thompson, *Environ. Sci. Technol.*, 2015, **49**, 5380–5389; (e) H. X. Li, G. J. Getzinger, P. L. Ferguson, B. Orihuela, M. Zhu and D. Rittschof, *Environ. Sci. Technol.*, 2016, **50**, 924–931.
- (a) A. Ohtaki, N. Sato and K. Nakasaki, *Polym. Degrad. Stab.*, 1998, **61**, 499–505; (b) A. Nawaz, F. Hasan and A. A. Shah, *FEMS Microbiol. Lett.*, 2015, **362**, 1–7; (c) M. Nevoralová, M. Koutný, A. Ujčić, Z. Starý, J. Šerá, H. Vlková, M. Šlouf, I. Fortelný and Z. Kruliš, *Front. Mater.*, 2020, **7**, 141; (d) Y. Tokiwa, B. P. Calabia, C. U. Ugwu and S. Aiba, *Int. J. Mol. Sci.*, 2009, **10**, 3722–3742.
- (a) A. Bhatia, R. K. Gupta, S. N. Bhattacharya and H. J. Choi, *J. Nanomater.*, 2012, **2012**, 1–11; (b) K. Halász, Y. Hosakun and L. Csóka, *Int. J. Polym. Sci.*, 2015, **2015**, 1–6; (c) J. Bota, M. Vukoje and Z. Hrnjak-Murgić, *Chem. Biochem. Eng. Q.*, 2018, **31**, 417–424.
- (a) C. L. Salgado, E. M. Sanchez, C. A. Zavaglia and P. L. Granja, *J. Biomed. Mater. Res., Part A*, 2012, **100**, 243–251; (b) M. Abedalwafa, F. Wang, L. Wang and C. Li, *Rev. Adv. Mater. Sci.*, 2013, **34**, 123–140; (c) Y. Ramot, M. Haim-Zada, A. J. Domb and A. Nyska, *Adv. Drug Delivery Rev.*, 2016, **107**, 153–162; (d) E. S. Permyakova, J. Polčák, P. V. Slukin, S. G. Ignatov, N. A. Gloushankova, L. Zajíčková, D. V. Shtansky and A. Manakhov, *Mater. Des.*, 2018, **153**, 60–70.
- (a) A. Yadav, S. Ghosh, A. Samanta, J. Pal and R. K. Srivastava, *Chem. Commun.*, 2022, **58**, 1468–1480; (b) K. S. Egorova, E. G. Gordeev and V. P. Ananikov, *Chem. Rev.*, 2017, **117**, 7132–7189; (c) N. Kamaly, B. Yameen, J. Wu and O. C. Farokhzad, *Chem. Rev.*, 2016, **116**, 2602–2663; (d) M. Abrisham, M. Noroozi, M. Panahi-Sarmad, M. Arjmand, V. Goodarzi, Y. Shakeri, H. Golbaten-Mofrad, P. Dehghan, A. S. Sahzabi, M. Sadri and L. Uzun, *Eur. Polym. J.*, 2020, **131**, 109701–109716; (e) J. Y. Park, G. Gao, J. Jang and D. W. Cho, *J. Mater. Chem. B*, 2016, **4**, 7521–7539; (f) B. Dellago, A. A. Altun, R. Liska and S. Baudis, *J. Polym. Sci.*, 2022, **61**, 143–154; (g) K. Liu, X. Jiang and P. Hunziker, *Nanoscale*, 2016, **8**, 16091–16156; (h) S. Bhowmick, A. V. Thanusha, A. Kumar, D. Scharnweber, S. Rother and V. Koul, *RSC Adv.*, 2018, **8**, 16420–16432; (i) P. Han, C. Liu, R. Staples, C. S. Moran, S. S. Ramachandra, M. N. Gomez-Cerezo and S. Ivanovski, *RSC Adv.*, 2022, **12**, 24849–24856.
- (a) O. Santoro and C. Redshaw, *Catalysts*, 2020, **10**, 210; (b) O. Santoro, X. Zhang and C. Redshaw, *Catalysts*, 2020, **10**, 800; (c) E. Fazekas, P. A. Lowy, M. A. Rahman, A. Lykkeberg, Y. Zhou, R. Chambenahalli and J. A. Garden, *Chem. Soc. Rev.*, 2022, **51**, 8793–8814; (d) M. Chen and

- C. Chen, *Chin. J. Chem.*, 2020, **38**, 282–286; (e) D. M. Lyubov, A. O. Tolpygin and A. A. Trifonov, *Coord. Chem. Rev.*, 2019, **392**, 83–145; (f) L.-J. Wu, W. Lee, P. K. Ganta, Y.-L. Chang, Y.-C. Chang and H.-Y. Chen, *Coord. Chem. Rev.*, 2023, **475**, 214847–214869; (g) J. Bhattacharjee, A. Sarkar and T. K. Panda, *Curr. Opin. Green Sustainable Chem.*, 2021, **31**, 100545; (h) S. Kaler and M. D. Jones, *Dalton Trans.*, 2022, **51**, 1241–1256; (i) M. Strianese, D. Pappalardo, M. Mazzeo, M. Lamberti and C. Pellecchia, *Dalton Trans.*, 2020, **49**, 16533–16550; (j) H. Wang, J. M. O. Cue, E. L. Calubaquib, R. N. Kularatne, S. Taslimy, J. T. Miller and M. C. Stefan, *Polym. Chem.*, 2021, **12**, 6790–6823; (k) W. A. Munzeiwa, B. O. Omondi and V. O. Nyamori, *Polym. Bull.*, 2024, **81**, 9419–9464; (l) S. Sagar, P. Nath, A. Ray, A. Sarkar and T. K. Panda, *Dalton Trans.*, 2024, **53**, 12837–12866; (m) W. Wang, *ACS Omega*, 2024, **9**, 29983–29993; (n) U. Yolsal, P. J. Shaw, P. A. Lowy, R. Chamenahalli and J. A. Garden, *ACS Catal.*, 2024, **14**, 1050–1074.
- 7 (a) T. Fuoco and D. Pappalardo, *Catalysts*, 2017, **7**, 64; (b) Y. Sarazin and J. F. Carpentier, *Chem. Rev.*, 2015, **115**, 3564–3614; (c) W.-H. Rao, L. Yu and J.-D. Ding, *Chin. J. Polym. Sci.*, 2023, **41**, 745–759; (d) I. Nifant'ev and P. Ivchenko, *Molecules*, 2019, **24**, 4117; (e) J.-F. Carpentier, *Organometallics*, 2015, **34**, 4175–4189; (f) E. Stirling, Y. Champouret and M. Visseaux, *Polym. Chem.*, 2018, **9**, 2517–2531.
- 8 (a) S. Gesslbauer, G. Hutchinson, A. J. P. White, J. Burés and C. Romain, *ACS Catal.*, 2021, **11**, 4084–4093; (b) X. Zhang, K. Chen, M. Chicoma, K. Goins, T. Prior, T. Nile and C. Redshaw, *Catalysts*, 2021, **11**, 1090; (c) C.-J. Chang, W. Lee, Y.-C. Liou, Y.-L. Chang, Y.-C. Lai, S. Ding, H.-Y. Chen, H.-Y. Chen and Y.-C. Chang, *Eur. Polym. J.*, 2022, **181**, 111651–111662; (d) S. R. Kosuru, Y. L. Chang, P. Y. Chen, W. Lee, Y. C. Lai, S. Ding, H. Y. Chen, H. Y. Chen and Y. C. Chang, *Inorg. Chem.*, 2022, **61**, 3997–4008; (e) S. R. Kosuru, F. J. Lai, Y. L. Chang, C. Y. Li, Y. C. Lai, S. Ding, K. H. Wu, H. Y. Chen and Y. H. Lo, *Inorg. Chem.*, 2021, **60**, 10535–10549; (f) J. Meimoun, C. Sutapin, G. Stoclet, A. Favrelle, P. Roussel, M. Bria, S. Chirachanchai, F. Bonnet and P. Zinck, *J. Am. Chem. Soc.*, 2021, **143**, 21206–21210; (g) M.-T. Chen, T.-H. Huang, F.-A. Yang and B.-H. Chen, *J. Organomet. Chem.*, 2022, **979**, 122493–122501; (h) Y. W. Lin, Y. C. Su, B. T. Ko, A. Datta and J. H. Huang, *J. Chin. Chem. Soc.*, 2023, **70**, 1065–1075; (i) E. N. Cooper, B. Averkiev, V. W. Day and P. E. Sues, *Organometallics*, 2021, **40**, 3185–3200; (j) A. M. McCollum, A. M. Longo, A. E. Stahl, A. S. Butler, A. L. Rheingold, T. R. Cundari, D. B. Green, K. R. Brereton and J. M. Fritsch, *Polyhedron*, 2021, **204**, 115233–115245; (k) E. Yue, F. Cao, J. Zhang, W. Zhang, Y. Jiang, T. Liang and W. H. Sun, *RSC Adv.*, 2021, **11**, 13274–13281; (l) P. K. Ganta, M. R. Teja, C. J. Chang, A. Sambandam, R. Kamaraj, Y. T. Chu, S. Ding, H. Y. Chen and H. Y. Chen, *Dalton Trans.*, 2023, **52**, 17132–17147; (m) P. K. Ganta, M. R. Teja, R. Kamaraj, Y.-R. Tsai, Y.-T. Chu, A. Sambandam, Y.-C. Lai, S. Ding and H.-Y. Chen, *Organometallics*, 2023, **42**, 3405–3417; (n) S. Impemba, I. Tozio, G. Roviello, S. Mameri, S. Dagorne and S. Milione, *Organometallics*, 2023, **42**, 921–932; (o) Y. W. Lin, Y. C. Su, B. T. Ko, A. Datta and J. H. Huang, *J. Chin. Chem. Soc.*, 2023, **70**, 1065–1075; (p) Z. Peng, H. Ahmed, G. Xu, X. Guo, R. Yang, H. Sun and Q. Wang, *Polym. Chem.*, 2023, **14**, 2174–2180; (q) V. Vaillant-Coindard, F. Chotard, B. Theron, C. Balan, J. Bayardon, R. Malacea-Kabbara, E. Bodio, Y. Rousselin, P. Fleurat-Lessard and P. L. Gendre, *Inorg. Chem.*, 2023, **62**, 7342–7352; (r) M. Wang, Z. Ding, B. Wang and Y. Li, *Polym. Chem.*, 2023, **14**, 45–54; (s) Y. Wongnongwa, S. Haesuwannakij, K. Udomsasporn, P. Chumsaeng, A. Watcharapasorn, K. Phomphrai and S. Jungsuttiwong, *Polymer*, 2023, **281**, 126065–126075; (t) S. Yimthachote and K. Phomphrai, *New J. Chem.*, 2023, **47**, 2701–2705; (u) M. Zang, W. Cao, X. Zhang, S. Liu and Z. Li, *Eur. Polym. J.*, 2023, **193**, 112103–112109; (v) S. Goswami, P. Mandal, S. Sarkar, M. Mukherjee, S. Pal, D. Mallick and D. Mukherjee, *Dalton Trans.*, 2024, **53**, 1346–1354; (w) X. Guo, G. Xu, R. Yang and Q. Wang, *J. Am. Chem. Soc.*, 2024, **146**, 9084–9095; (x) K.-M. Lin, Y.-H. Lin, C.-A. Cheng, H.-Y. Chen and L.-C. Liang, *Polyhedron*, 2024, **255**, 116975–116979; (y) C. Nakornkhet, S. Kamavichanurat, W. Joopor and P. Hormnirun, *Polym. Chem.*, 2024, **15**, 1660–1679; (z) Y. Rusconi, M. C. D'Alterio, C. De Rosa, Y. Lu, S. M. Severson, G. W. Coates and G. Talarico, *ACS Catal.*, 2024, **14**, 318–323; (aa) P. Sumrit, S. Kamavichanurat, W. Joopor, W. Wattanathana, C. Nakornkhet and P. Hormnirun, *Dalton Trans.*, 2024, **53**, 13854–13870.
- 9 H. C. Tseng, M. Y. Chiang, W. Y. Lu, Y. J. Chen, C. J. Lian, Y. H. Chen, H. Y. Tsai, Y. C. Lai and H. Y. Chen, *Dalton Trans.*, 2015, **44**, 11763–11773.
- 10 M. C. Chang, W. Y. Lu, H. Y. Chang, Y. C. Lai, M. Y. Chiang, H. Y. Chen and H. Y. Chen, *Inorg. Chem.*, 2015, **54**, 11292–11298.
- 11 P. K. Ganta, C.-J. Chang, H.-Y. Chen, R. Kamaraj, A. Sambandam, Y.-C. Lai, Y.-T. Chu, S. Ding and H.-Y. Chen, *Organometallics*, 2023, **42**, 2856–2866.
- 12 A. I. Fedulin, Y. F. Oprunenko, A. R. Egorov, A. V. Churakov and K. V. Zaitsev, *J. Organomet. Chem.*, 2024, **1017**, 123278–123285.
- 13 E. Block, V. Eswarakrishnan, M. Gernon, G. Ofori-Okai, C. Saha, K. Tang and J. Zubieta, *J. Am. Chem. Soc.*, 1989, **111**, 658–665.
- 14 L. Yang, D. R. Powell and R. P. Houser, *Dalton Trans.*, 2007, 955–964.
- 15 T. Majid, M. J. Heeg, M. Bailey, D. G. Dick, R. Kumar, D. G. Hendershot, H. Rahbarnoohi and J. P. Oliver, *Organometallics*, 1995, **14**, 2903–2917.
- 16 (a) J. A. Francis, S. G. Bott and A. R. Barron, *J. Chem. Soc., Dalton Trans.*, 1998, 3305–3310; (b) L. S. Baugh and J. A. Sissano, *J. Polym. Sci., Part A: Polym. Chem.*, 2002, **40**, 1633–1651.

- 17 J. Lewiński, P. Horeglad, E. Tratkiewicz, W. Grzenda, J. Lipkowski and E. Kolodziejczyk, *Macromol. Rapid Commun.*, 2004, **25**, 1939–1942.
- 18 M. C. Chang, W. Y. Lu, H. Y. Chang, Y. C. Lai, M. Y. Chiang, H. Y. Chen and H. Y. Chen, *Inorg. Chem.*, 2015, **54**, 11292–11298.
- 19 (a) T. Ooi, M. Takahashi, M. Yamada, E. Tayama, K. Omoto and K. Maruoka, *J. Am. Chem. Soc.*, 2004, **126**, 1150–1160; (b) T. Ooi, M. Takahashi and K. Maruoka, *Angew. Chem., Int. Ed.*, 1998, **37**, 835–837; (c) T. Ooi, M. Takahashi and K. Maruoka, *J. Am. Chem. Soc.*, 1996, **118**, 11307–11308.
- 20 M. Taghiof, M. J. Heeg, M. Bailey, D. G. Dick, R. Kumar, D. G. Hendershot, H. Rahbarnoohi and J. P. Oliver, *Organometallics*, 1995, **14**, 2903–2917.
- 21 (a) K. Maruoka, T. Miyazaki, M. Ando, Y. Matsumura, S. Sakane, K. Hattori and H. Yamamoto, *J. Am. Chem. Soc.*, 1983, **105**, 2831–2843; (b) D. J. Dixon, A. C. Foster, S. V. Ley and D. J. Reynolds, *J. Chem. Soc., Perkin Trans. 1*, 1999, 1631–1633; (c) T. Murai, T. Mizutani, Y. Ogino, Y. Fujiwara and S. Kato, *Phosphorus, Sulfur Silicon Relat. Elem.*, 2008, **136**, 561–564.
- 22 R. Kumar, V. S. J. de Mel, M. L. Sierra, D. G. Hendershot and J. P. Oliver, *Organometallics*, 1994, **13**, 2079–2083.
- 23 R. Kumar, V. S. J. De Mel and J. P. Oliver, *Organometallics*, 1989, **8**, 2488–2490.
- 24 (a) T.-Y. Lin, Y.-C. Liou, T. B. Halima, S.-Y. Huang, R. Kamaraj, H.-C. Tseng, S. Ding, H.-Y. Chen and C.-M. Lee, CCDC 2386781: Experimental Crystal Structure Determination, 2025, DOI: [10.5517/ccdc.csd.cc2l3my9](https://doi.org/10.5517/ccdc.csd.cc2l3my9); (b) T.-Y. Lin, Y.-C. Liou, T. B. Halima, S.-Y. Huang, R. Kamaraj, H.-C. Tseng, S. Ding, H.-Y. Chen and C.-M. Lee, CCDC 2386782: Experimental Crystal Structure Determination, 2025, DOI: [10.5517/ccdc.csd.cc2l3mzb](https://doi.org/10.5517/ccdc.csd.cc2l3mzb); (c) T.-Y. Lin, Y.-C. Liou, T. B. Halima, S.-Y. Huang, R. Kamaraj, H.-C. Tseng, S. Ding, H.-Y. Chen and C.-M. Lee, CCDC 2386783: Experimental Crystal Structure Determination, 2025, DOI: [10.5517/ccdc.csd.cc2l3n0d](https://doi.org/10.5517/ccdc.csd.cc2l3n0d); (d) T.-Y. Lin, Y.-C. Liou, T. B. Halima, S.-Y. Huang, R. Kamaraj, H.-C. Tseng, S. Ding, H.-Y. Chen and C.-M. Lee, CCDC 2468931: Experimental Crystal Structure Determination, 2025, DOI: [10.5517/ccdc.csd.cc2nw3ym](https://doi.org/10.5517/ccdc.csd.cc2nw3ym).